Support to ITER Diagnostic Design

Contract: EFDA 01.649

Task: CXRS and MSE
(deliverables D6 and D7)

Active Charge Exchange Recombination Spectroscopy (CXRS) and Beam Emission Spectroscopy (BES + MSE) with Diagnostic Neutral Beam (DNB)

Manfred von Hellermann

December 2003

FOM Institute for Plasma Physics Rijnhuizen
Association Euratom-FOM, Trilateral Euregio Cluster
3430 BE Nieuwegein NL

Summarising abstract

A report is given on the status and recent developments of Active Beam Spectroscopy for ITER issues with specific emphasis on:

1) **Optimisation of upper port viewing system based on physics discussion**
2) **Demonstration of feasibility of implementation of viewing system**
3) **Motivation for equatorial viewing port system for poloidal and toroidal velocity measurements**
4) **Proposed use of DNB periscopes for MSE measurements**
5) **Assessment of physics merits of negative ion source based DNB compared to positive ion source system**
6) **Physics merits for a tilted DNB reaching magnetic axis**
7) **Description of pilot experiments and envisaged further development work**

Acknowledgement

This report is based on multiple discussions and contributions by members of the Active Beam Spectroscopy Working Group, in particular I would like to thank:

Artur Malaquias, IT Garching
Chris Walker, IT Garching
Hans Falter, IPP Garching
Ron Hemsworth, CEA Cadarache
Philippe Lotte, CEA Cadarache
Sergei Tugarinov Triniti Troitsk
Nick Hawkes ,UKAEA Culham Laboratory
Martin O'Mullane, UKAEA Culham Laboratory
Roger Jaspers, FOM Institute Rijnhuizen
Klaus-Dieter Zastrow, UKAEA, Culham Laboratory

Content

1. Introduction and status of CXRS feasibility studies for ITER

A comprehensive package of active beam based spectroscopy tools for ITER has been developed and evaluated. The feasibility study encompasses CXRS (*Charge Exchange Recombination Spectroscopy*) for the measurement of the main impurity ion densities (including helium ash), ion temperatures and toroidal as well as poloidal plasma rotation. *Beam Emission Spectroscopy* is proposed as indispensable cross-calibration tool for absolute local impurity density measurements[1] and also for the continuous monitoring of the neutral beam power deposition profile. Finally, a full exploitation of the '*Motional Stark Effect*' pattern is proposed to deduce local pitch angles, total magnetic fields and possibly radial electric fields.

More recently[2],[3], a further promising application has been proposed, that is a study of slowing-down alpha particles in the energy range of 0.1 to 0.6 MeV and 1.6 to 2.4 MeV respectively making use of the *2.2MW 100 keV/amu DNB (Diagnostic Neutral Beam)* and the *17MW 500keV/amu HNB (Heating Neutral Beam)*. An important asset of the proposed slowing-down scheme is the potential investigation of anisotropic features in the alpha velocity distribution function making use of top and equatorial observation periscopes.

Performance studies and estimates of expected spectral signal-to-noise ratios are based on atomic modelling[4] of neutral beam stopping and emissivities for CXRS, BES and background continuum radiation as well as extrapolations from present CXRS diagnostic systems. Single high-étendue and high-resolution spectrometers[5] for each radial channel are proposed for thermal CXRS and BES/MSE and high-étendue broad-band spectrometers for CXRS on slowing-down features.

The concept of integrated data evaluation procedures plays a pivotal role for a feasible and successful application of active beam diagnostics on ITER. The issue of measuring the helium ash content and part of the slowing-down velocity function is strongly interwoven with the ability of assessing at the same time all complementary ion densities (including bulk ions) and ion temperatures. The consistency of diamagnetic energy data with spectroscopic reconstructions from electron and ion pressure profiles, or the consistency of measured thermo-nuclear neutron rates with modelled predictions from measured ion temperature and deuteron/triton density profiles belong to standard prediction packages (TRANSP, CHEAP) in present day experiments (e.g. JET). Each of these reconstructions requires a high degree of data accuracy and local resolution which cannot be provided by any other non-active, and hence non-localised, diagnostic method.

A key issue for the viability of the proposed active beam spectroscopy package is the survival probability of the first mirror in its periscopes. Studies of metallic mirrors deposition[6] and today's experiments on sputtering processes addressing reflection values and polarisation characteristics have given first results[7].

---

[1] M.von Hellermann et al. Proc.Adv.Diag.for Magn. & Inert. Fus. Varenna 2001,205-208, Plenum Publ. N.Y.

[2] M.von Hellermann et al. Proc. 4'th ITPA Topic Group Meeting on Diagnostics, Padova ,17-21 February, 2003

[3] S.Tugarinov et al. RF Meeting on ITER/BPX Relevant Diagnostic Developments, St. Petersburg,15 July 2003

[4] c.f. H.P.Summers et al. Physica Scripta **T92**,80(2001) and http://adas.phys.strath.ac.uk/

[5] S.Tugarinov et al. Rev.Sci.Instr., 74,2075, 2003

[6] A.Malaquias et al. Proc. 5'th ITPA Topic Group Meeting on Diagnostics, St.Petersburg, 12-18 July, 2003

[7] K.Vukolov et al. Proc. 4'th ITPA Topic Group Meeting on Diagnostics, Padova ,17-21 February, 2003

2. Layout of periscopes and radial resolutions

Following the first feasibility study presented in 2001[8] considerable progress has been made in the layout of CXRS periscopes, ray-tracing of the optical imaging system of the DNB path onto the receiving fibre bundle and finally specification of spectral instrumentation. The original scheme of having only a single top-port periscope with a poloidal view on the DNB, which had been chosen in order to minimise the path lengths of the lines-of-sight thus minimising the underlying background continuum radiation, had to be extended by additional equatorial periscopes. In fact, two top-port periscopes had been considered in a first iteration, that is, one periscope for the core- and one for the edge-region. The latter was chosen to avoid a direct view from the top-port position into the divertor region, where an enhanced level of background line emission is expected.

The main reason for adding equatorial periscopes (cf. Figs.1, 2, 3) was the need of a high radial resolution ($\leq a/20$) across the entire DNB path length from separatrix to plasma core. The resolution is essentially determined by the geometric intersection of line of sight and DNB and the variation of minor plasma radii in region of intersection path. The poloidal viewing fan from the top port provides only sufficient resolution in the very core region and deteriorates towards the edge due to field geometry (cf. Figs.4 and 5).

A further motivation for the proposed two additional equatorial periscopes with downward and upward views respectively was the improved option for measuring low poloidal velocities with sufficient accuracy (cf. Fig.7).

Although the two equatorial periscopes will be able to cover the entire minor radius range ($0<r/a<1$) and also be suitable for most of the physics tasks, the top-port periscope is retained, and a combination of top- and equatorial observation ports is proposed. The combination of the two periscope systems offers several unique features:

The pitch-angle of the magnetic field, as determined by a MSE measurement of the DNB Stark spectrum is more favourable for the top-port position (c.f. section 5).

Helium-ash measurements are potentially affected by ‘plume’ features in the HeII spectrum. A simultaneous measurement of the CX HeII spectrum in directions approximately parallel and perpendicular to the magnetic field will allow the unique extraction, or suppression, of that feature. Moreover, the poloidal view from the top-port minimises the line-of-sight path length through the plasma and hence the continuum radiation.

For slowing-down alphas anisotropic loss-mechanisms are expected, and for an experimental verification of this effect the two observation ports are required. Each periscope will measure the velocity distribution function or the corresponding CX spectrum in the direction of observation that is parallel and perpendicular to the magnetic field. Other anisotropic features may, for example, occur in ion temperature measurements in beam heated plasmas.

[8] “CXRS for ITER” M von Hellermann et al. in the Final Report on EFDA Contracts 00-558,00-599 and 00-560, May 2001

A common feature of all periscope locations is the ability to measure the D-alpha beam emission spectra along the DNB path, which is considered to be an indispensable tool for absolute calibrations of CX ion densities (cf. section 6). Moreover, the Doppler-shift of the D-alpha spectrum provides a convenient tool for the verification of the precise intersection radius of line-of-sight and DNB. This technique is used at many of the present CXRS diagnostic systems, ensuring typical radial accuracies better than 1% of the major tokamak radius. For the case of ITER this corresponds to radial accuracies of about 0.08m. The latter capability is also an essential feature in context with magnetic measurements involving the total magnetic field[9] (cf. section 5).

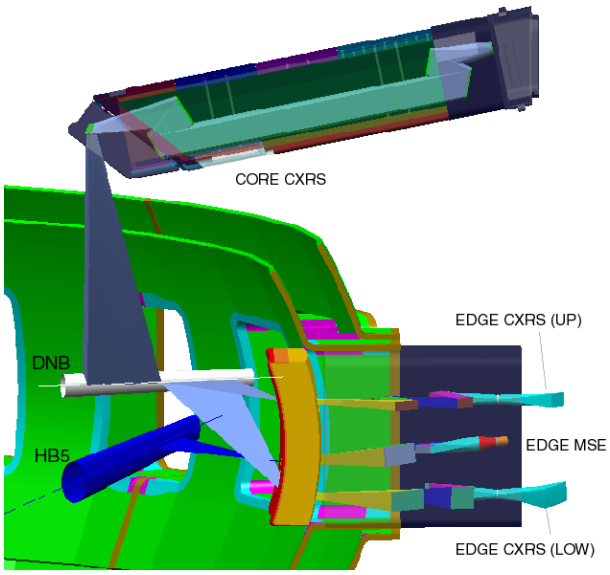

Fig.1 Layout of top and equatorial CXRS and BES periscopes. Courtesy IT Garching

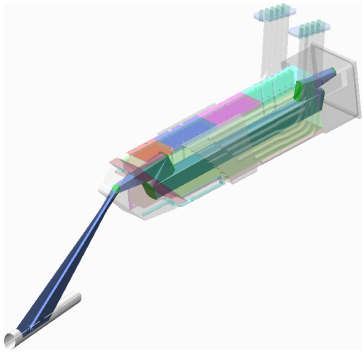

Fig.2a. Implementation of top-DNB periscope in upper port plug. Courtesy IT Garching.

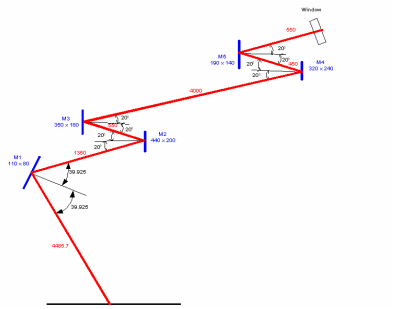

Fig.2b Ray-tracing of upper port periscope onto DNB.

Table I. Details of proposed optical components for top port periscope:

#	Type	Glass	Radius Y	Radius X	Thickness	Diameter
Obj	STANDARD				4485.7	1000.0
1	STANDARD	MIRROR	Infinity		1350.0	106.9
2	BICONICX	MIRROR	-2314.95	-3320.25	550.0	444.4
3	STANDARD	MIRROR	Infinity		4000.0	365.2
4	BICONICX	MIRROR	-2151.83	-1594.83	450.0	353.6
5	STANDARD	MIRROR	Infinity		500.0	204.2
6	STANDARD	QUARTZ	192.63		30.0	139.0
7	STANDARD		3957.76		175.7	135.0
Image	STANDARD		Infinity	Infinity		63.0

[9] R.Wolf et al. "Motional Stark Effect Measurements of the Local ICRH Induced Diamagnetism in JET Plasmas" Nuclear Fusion, 33, 1835(1993)

An important feature of the present conceptual design is to ensure multi-tasking of the proposed periscopes. Once the detected light has been carried through beyond the biological wall via the periscope labyrinth system and then a multi-fibre bundle, it can be split up by beam-splitters onto several instruments (cf.Fig.6).

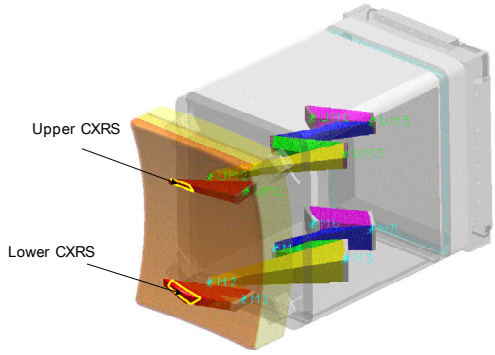

Fig.3 a. Implementation of CXRS periscopes in equatorial and mirror labyrinth.

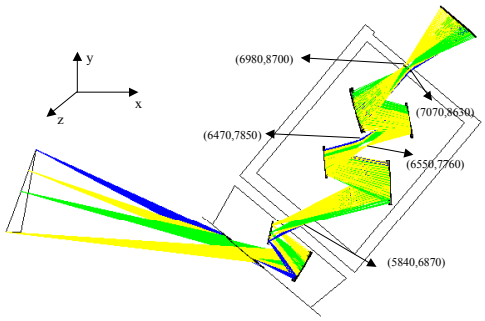

Fig.3b Raytracing of lower equatorial port periscope. For details of components see table below.

Table II Optical components for equatorial port periscopes:

Component	width	Height	Focal radius longitudinal	Focal radius transversal	X	Y	z	Angle to x
M1	350	90	950	1100	5873	6441	1070	-29
M2	260	40	INFINITY	INFINITY	5493	6781	1070	170
M3	360	120	1600	1100	6833	7331	1070	2.3
M4	310	70	2600	2600	6103	7551	1070	186.3
M5	250	130	2500	2200	7063	8091	1070	11.6
M6	300	170	1200	1200	6453	8161	1070	198

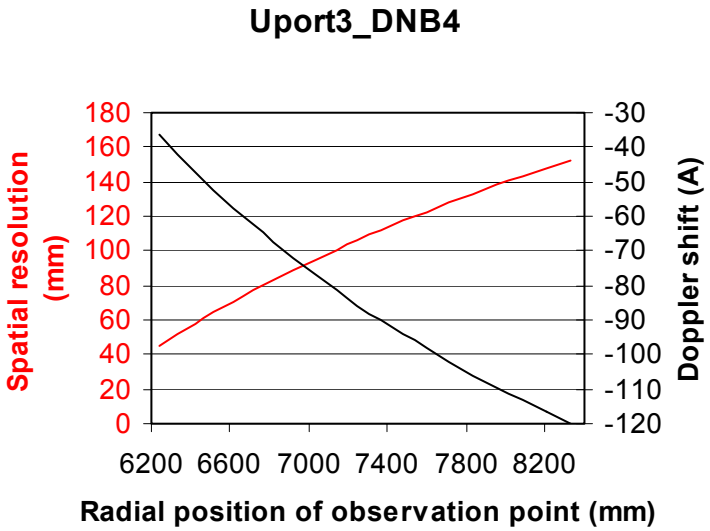

Fig.4 Radial resolution for top periscope (red trace) and Doppler shift of DNB D-alpha spectrum (black trace). (cf.A.Malaquias)

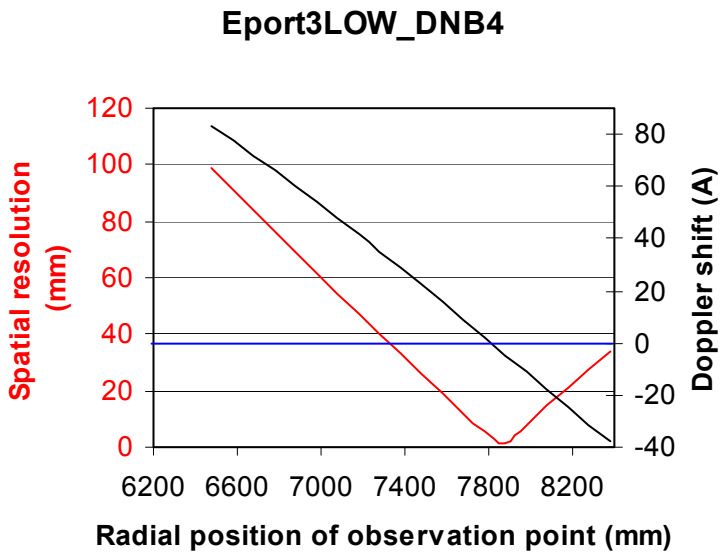

Fig.5 Radial resolution of equatorial periscopes. Black trace: Doppler-shift of BES-DNB. Red trace: Radial resolution (c.f. A.Malaquias).

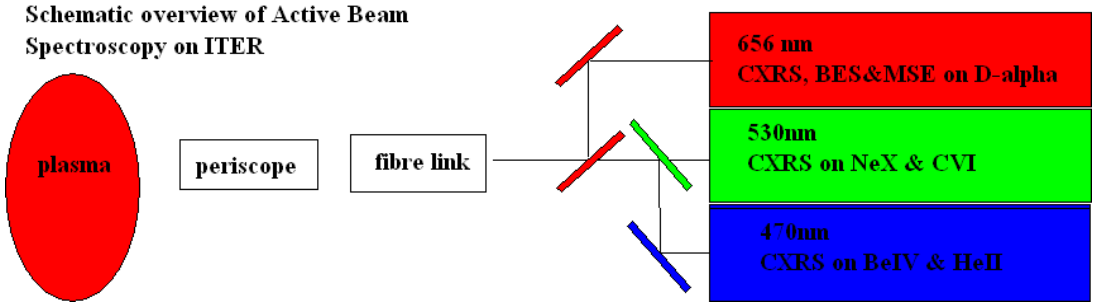

Fig.6a Schematic layout of CXRS/BES/MSE spectroscopic instrumentation. Multi-tasking of periscopes for simultaneous evaluation of CXRS (impurity and bulk ions), BES on injected neutrals and finally for MSE ratiometry. The instruments are high-étendue, high-resolution échelle-spectrometers (F/3, 2.5Å/mm)(cf. S.Tugarinov). For maximum throughput single fibres, which represent one radial channel each, will be imaged onto one spectrometer and camera.
The beam splitters shown could be edge filters which would pass on the remaining spectra with high efficiency.
An alternative scheme would be an active colour-filter assembly at the output plane of one single échelle grating spectrometer and using different diffraction orders for each wavelength regime.

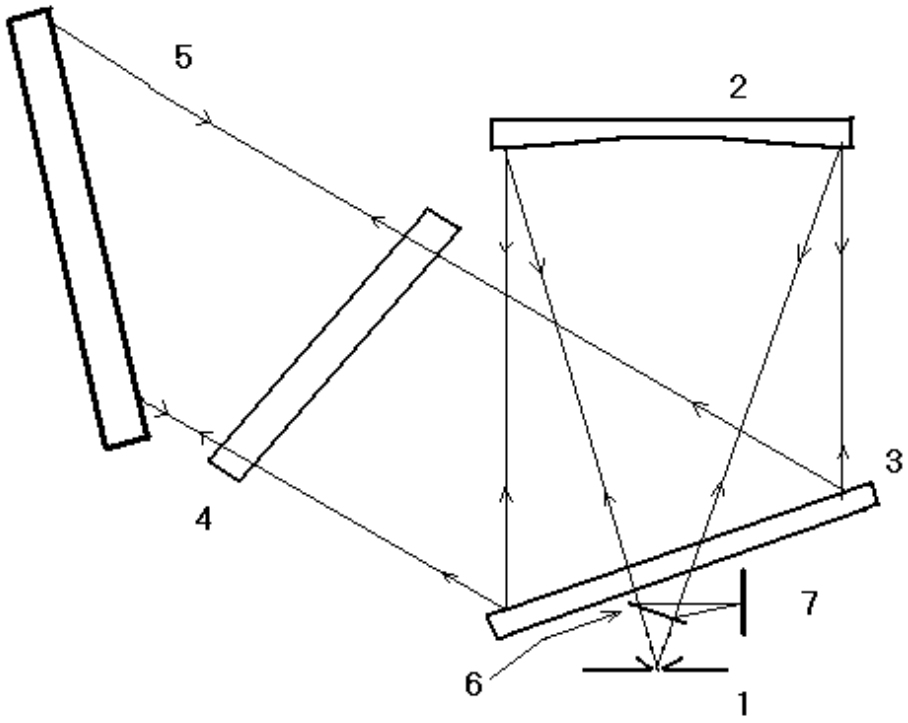

Fig.6b Schematic description of high resolution TRINITI spectrometer. 1 entrance slit, 2 spherical mirror, 3 flat mirror with hole, 4 correction element, 5 echelle grating, 6 deflecting flat mirror, 7 image plane

3. Poloidal and toroidal rotation measurements

For ITER very low poloidal rotation velocities are expected, which may be of the order 5km/s or less. This will require spectral resolutions, or wavelength accuracies <0.02 Å corresponding to 1km/s. The region of measurable velocities will be limited to the very edge region, where strong pressure gradients can be associated with radial electrical fields and hence measurable and non-zero poloidal velocities. In addition to the challenge of measuring tiny Doppler shifts, the narrow sheath of poloidal velocities requires also adequate spatial resolution. Another problem arises by a potential error source in Doppler shift measurement caused by the need of a reliable absolute wavelength reference. For this reason we have proposed a dual equatorial periscope system with opposed poloidal components. Making use of the dual periscope observation we obtain for the difference and sum of top and bottom equatorial periscope and their respective Doppler shifts:

$$\Delta\lambda_{top} - \Delta\lambda_{bottom} = 2 \cdot \lambda_0 \cdot v_{poloidal} \cdot \sin\alpha / c$$

and for the toroidal component:

$$\Delta\lambda_{top} + \Delta\lambda_{bottom} = 2 \cdot \lambda_0 \cdot v_{toroidal} \cdot \cos\alpha / c$$

The angle α=7.5° is the angle between equatorial periscope viewing fan and equatorial plane. The actual Doppler-shifts are derived from spectral least-square analysis of dominant CX spectra, which provide peak-positions and their respective statistical errors. Signal to noise studies on achievable poloidal velocity resolutions

are based on simulated CVI CX spectra including noise numbers from underlying continuum background. Fig.7 shows the expected error in deduced poloidal velocities as a function of the CVI-spectral amplitude error, in the range up to 0.2%. This statistical amplitude error corresponds to the spectral error expected close to the boundary region (cf. Fig.8). The spectral amplitude and position error is based on the fluctuation of underlying continuum radiation level expected for ITER plasma conditions with $n_e=10^{20}m^{-3}$, $T_e=20keV$ and $<Z_{eff}>=1.6$ (for details see Ref. 8).

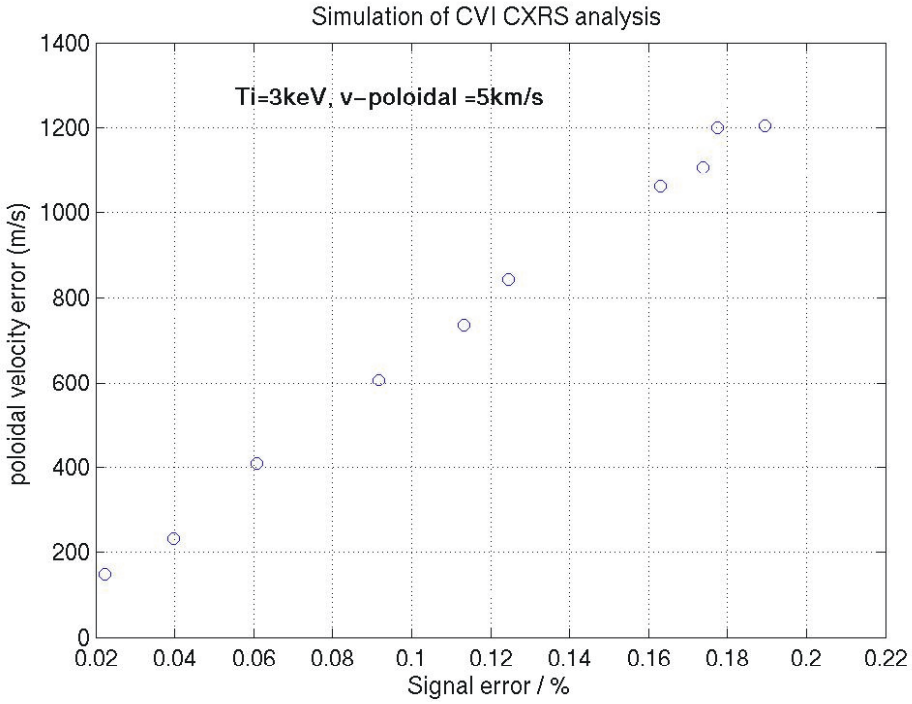

Fig.7 Error analysis for poloidal velocity measurements based on simulated CVI spectra. For the ITER edge region a SNR>1000 is expected for the measurement of the CX-CVI spectrum (see also Fig.8). A statistical error in the spectral amplitude at half-maximum of the order 0.1% corresponds to an error in deductible poloidal rotation of 0.6 km/sec.

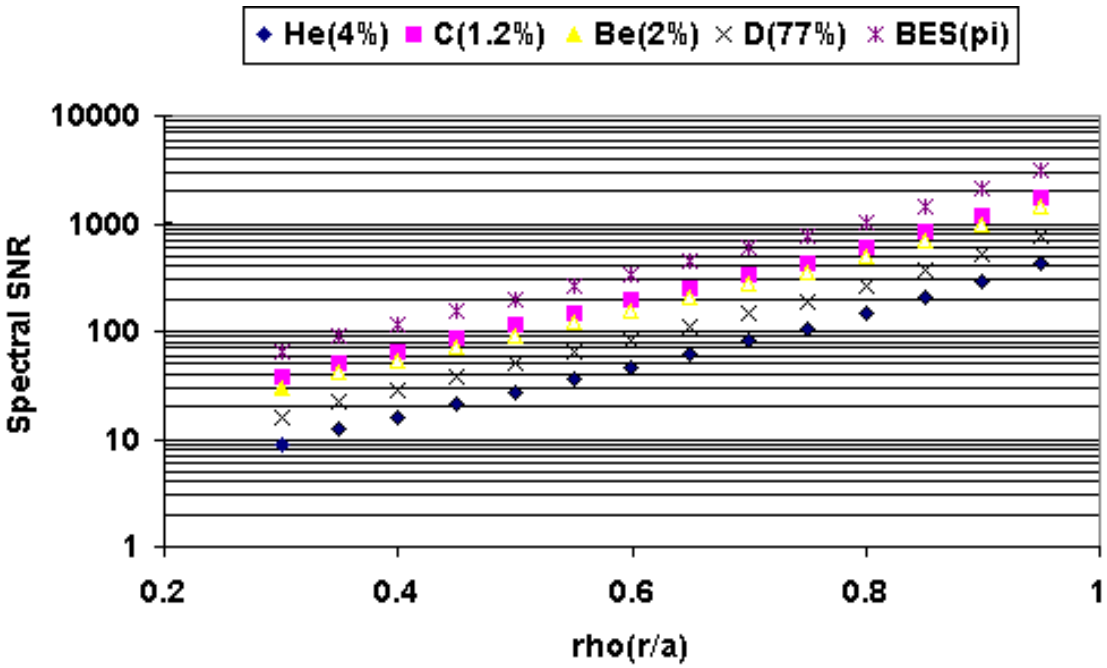

Fig.8 Spectral signal-to-noise ratio at half maximum for main light impurities (He,Be,C) and also bulk ions(D or T). The high SNR for the BES signal (see Fig.10) benefits from the increase of Q_{BES} with energy and also from the fact that atomic physics symmetries reduce the number of free amplitude parameters in the BES spectrum to the sigma and pi group respectively.

4. Beam Emission Spectroscopy

Beam Emission Spectroscopy on D-alpha spectra emitted by injected neutral beams has since its first description (cf.[10],[11]) evolved to a level where it can be used routinely as collateral tool to CXRS measurements. For the case of the ITER CXRS system effective BES emission rates, which increase strongly with beam energy (see Figs.9a, 9b and 9c), lead to spectral amplitudes far above the expected noise level of the continuum radiation background. Note, that for accurate atomic, i.e. collisional radiative, modelling of emission rates a full description of the background plasma data is required (e.g. n_e, T_e, c_z).

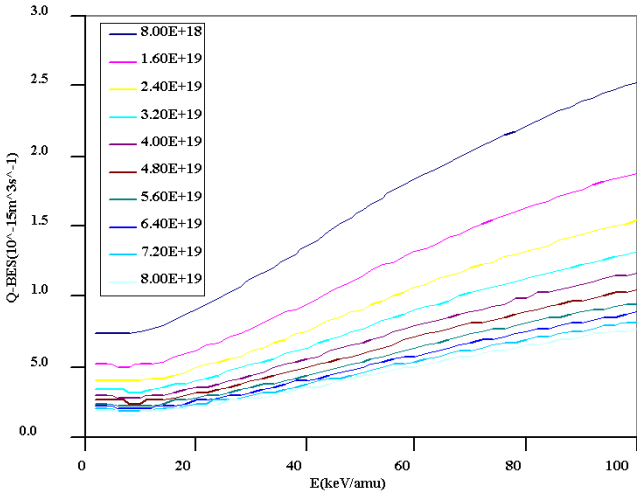

Fig.9a *Effective BES emission rate versus neutral beam energy in electron density range between $0.8{\cdot}10^{19}m^{-3}$ and $8{\cdot}10^{19}m^{-3}$. Data are from ADAS ADF 309 (c.f. Ref. 3)*

A synthetic spectrum for the top periscope geometry (Fig.10) shows the respective amplitudes of the BES Motional Stark feature and the neighbouring broad CX feature representing the bulk deuterium ions. The angles between lines of sight and DNB (cf. Fig. 12) lead to clear separations of BES CXRS components.

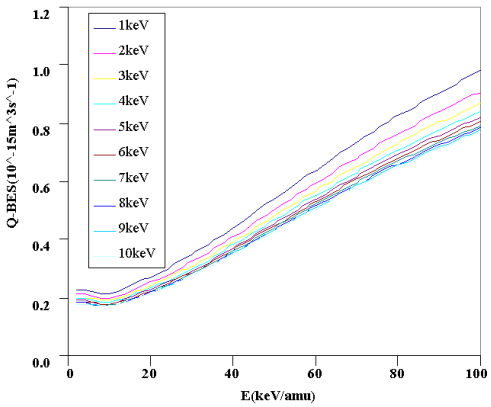

Fig9b Effective BES emission rate versus neutral beam energy and target ion temperature. N_e=810$^{19}m^{-3}$

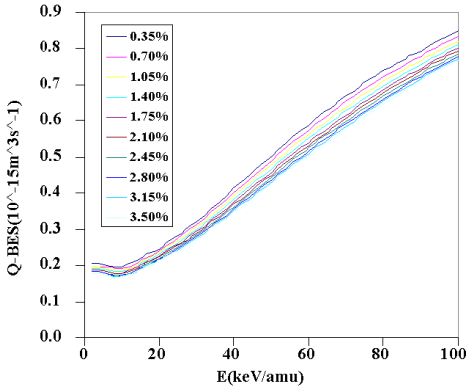

Fig.9c Effective BES emission rate versus beam energy and C^{6+} concentration for $N_e=8{\cdot}10^{19}m^{-3}$, T_i=10keV

[10] W.Mandl et al. 'Beam Emission Spectroscopy as a Comprehensive Plasma Diagnostic Tool' Plasma Phys. Contr. Fusion, **35**,1373, 1993

[11] H.Anderson et al.'Neutral beam stopping and emission in fusion plasmas I: deuterium beams', Plasma Physics and Contr. Fusion **42**,781-806(2000)

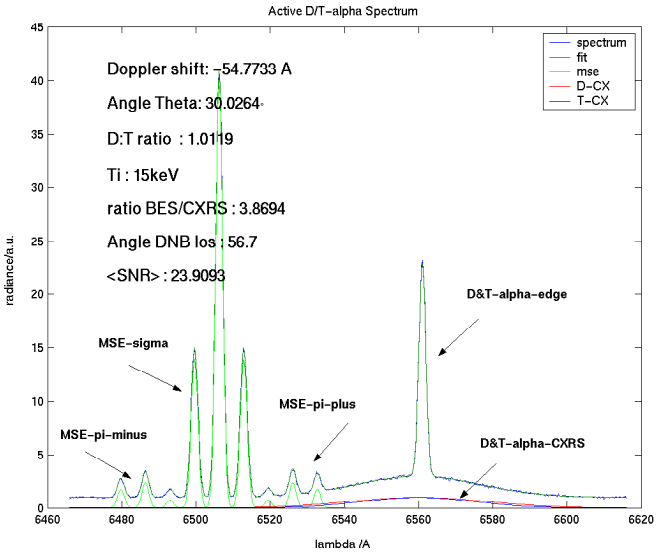

Fig.10 Simulated spectra for the Doppler-shifted BES and CXRS D-alpha line for the central top-port view on the DNB. The narrow D-alpha-edge spectrum at 6561Å is added as a wavelength marker. For the actual measurement, beam modulation, and hence background suppression for edge line emission and continuum radiation, is proposed. The SNR for the spectrum at half maxiumum for bulk ion CX is 24, and for BES(π)>60 corresponding to amplitude errors of 4% and 1.5% errors respectively.

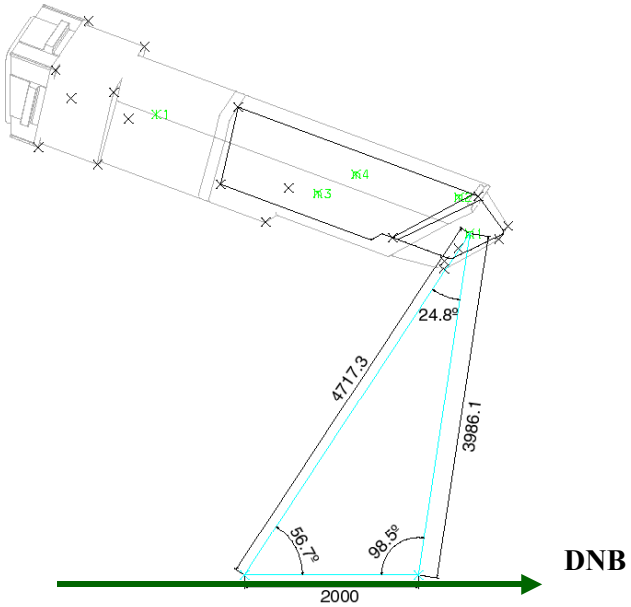

Fig.11 Angles between top-port lines of sight *and DNB ranging from 56.7° and 81.5° lead to Doppler shifts of the BES spectrum (see also Fig.4) clearly separated from the un-shifted edge line.*

5. Proposal for a DNB based Motional-Stark-Effect Diagnostic based on Ratiometry

The present understanding is that both the ITER DNB and HNB MSE[12] patterns should be exploited for maximum information on local magnetic fields, and, should ultimately enable the deduction of the current profile. A major concern in the feasibility of a workable MSE diagnostic is the preservation of the polarisation status of the detected light following its path through the labyrinth system of the periscopes. A recent study[13] has demonstrated that both polarisation status and polarisation dependent reflectivity will suffer from coatings on the original metallic mirror surfaces. Keeping the angles of incidence below 30° these effects can be minimised on the penalty that low angles of incidences imply a greater number of relay mirrors in the periscope labyrinth. To which degree those deteriorating effects can be calibrated in situ should be addressed in dedicated experiments (see also final remarks on this subject in the conclusion).

The following section summarises briefly the potential use of ports chosen in connection with the DNB and which would allow MSE measurements based on a pure line-ratio ("ratiometry") method rather than a measurement of the polarisation angle of – say the π-component – of the Stark multiplet. Since the measurement of the beam emission intensities is an absolute must for the CXRS evaluation (see section 6), it makes sense to explore the option of deriving pitch angle data from intensity ratios, which is a free spin-off of the BES data.. This scheme as proposed on the 2nd ITPA Meeting at San Diego in 2002[14] is to use MSE-ratiometry as complementary method to the usual MSE-polarimetry. MSE-ratiometry relies on the ratio of sigma- and pi-components in the Stark spectrum[15], which follows a dipole radiation pattern. The angle ϑ between lines-of-sight and local Lorentz vector ($\mathbf{E_{Lorentz}=v_{DNB}xB_{total}}$), determines the sensitivity for changes in local pitch-angle.

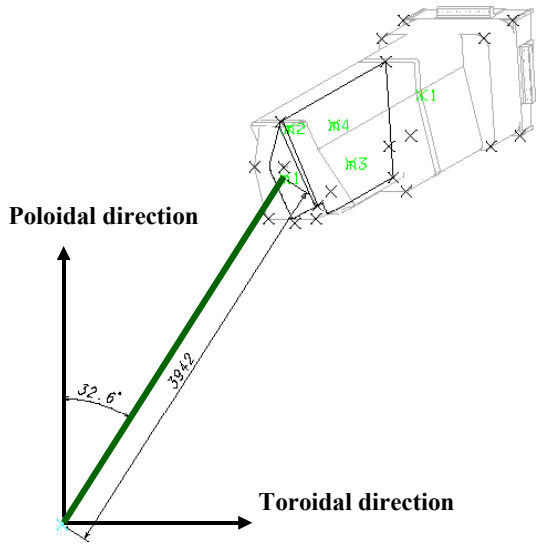

Fig.12a View from Top port(section 3) onto DNB showing angle between l.o.s. and Lorentz vector at magnetic axis and also potential toroidal and poloidal rotation components(c.f. A.Malaquias)

[12] N Hawkes et al. "Some Issues Affecting the Performance of the ITER MSE System" , 5th ITPA Meeting on Diagnostics , St. Petersburg, July 2003

[13] A.Malaquias et al. , "Polarisation and reflectivity changes on mirror based viewing systems during long pulse operation", 5th ITPA Meeting on Diagnostics , St. Petersburg, July 2003

[14] "Progress on CXRS and BES for ITER" M von Hellermann et al., 2nd ITPA Meeting on Diagnostics, San Diego , March 2002

[15] Note: A pilot experiment for this technique is currently prepared at TEXTOR

The intensity ratio of the σ and π-components is given by:

$$\frac{I_\pi}{I_\sigma} = \frac{\sin^2 \vartheta}{1+\cos^2 \vartheta}$$

For a circular poloidal magnetic flux geometry with: $q = \frac{B_{tor} \cdot r}{B_{pol} \cdot R_0}$, where B_{pol} is the poloidal field, B_{tor} the toroidal field, r the minor radius and R_0 the major radius, the angle theta can be expressed by $\vartheta = \vartheta_0 + a\tan\left[\frac{r}{q \cdot R_0}\right]$. Here the angle ϑ_0 is the angle between the vertical direction and central line-of-sight. Resolving for q as a function of the ratio $P = I_\pi / I_\sigma$ we obtain:

$$q(\rho) = \frac{\rho \cdot a}{R_0} \cot\left[a\tan\left\{\sqrt{\frac{2 \cdot P}{1-P}}\right\} - \vartheta_0 \right]$$

For the top-port periscope the angle ϑ_0 is 32.6° and for the lower and upper equatorial port periscopes 97.5° and 82.5° respectively. The plasma current is such that the angles are additive. The range of P values depends on the geometry and the actual q-profile. For the following simulation we have assumed a parabolic q-profile, and explored the range of parameters for the top-port and the lower equatorial port periscope (ϑ_0=97.5°). The upper equatorial periscope is not suitable, because the ratio P changes less than 2% over the radius.

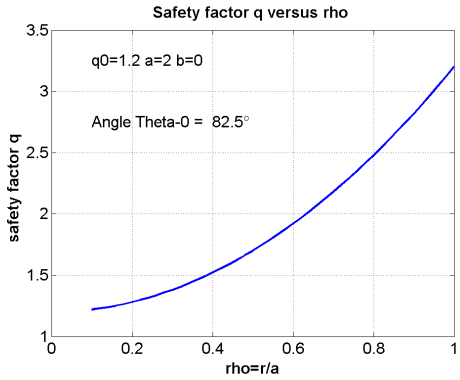

Fig.12b . 'Normal' q-profile case with parabolic shape and q>1 on the magnetic axis:

$$q = q_0 + a \cdot \rho^2 + b \cdot \rho^4$$

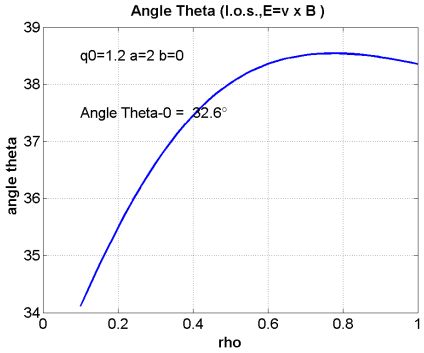

Fig. 12c. Changes of angle ϑ for top-port observation for positive shear q-profile (cf.Fig.12a).

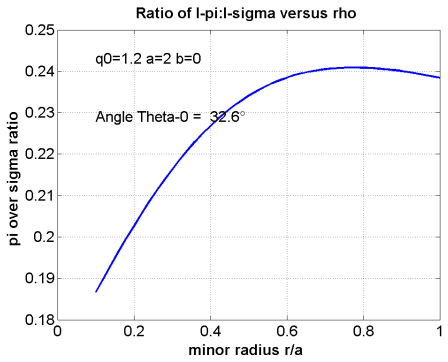

Fig. 12c Ratio P for top-port configuration

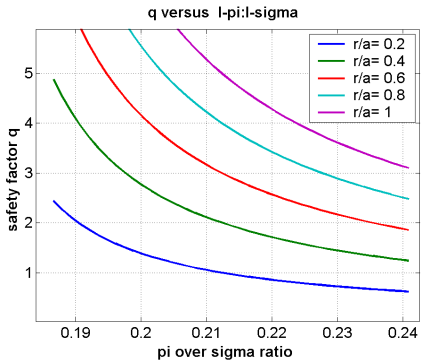

Fig.12d q-derived from ratio P for five radial positions. Top-port-periscope

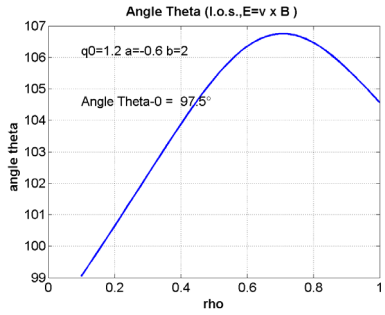

Fig.13a Changes of angle theta for lower equatorial periscope.

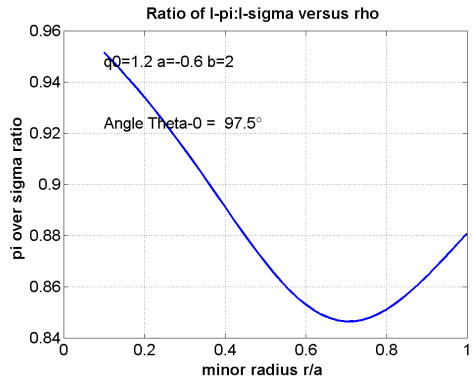

Fig.13b Ratio p for lower equatorial periscope

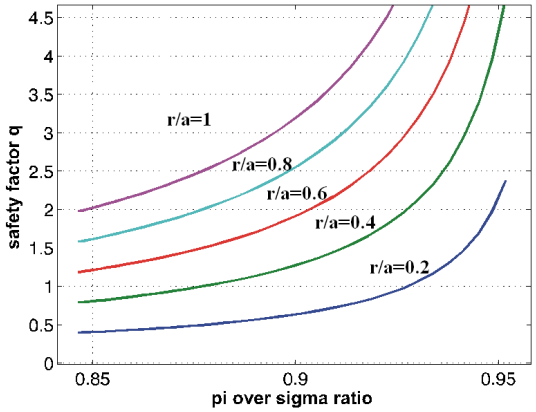

Fig. 13c q derived from ratio p for five radial positions. Lower equatorial periscope

MSE and total magnetic field measurements

A further potential use of the DNB induced Doppler-shifted Balmer-alpha spectrum is the highly resolved MSE pattern providing precise local Lorentz fields. For a radially injected DNB the local field strength is given by:

$E_{Lorentz} = v_{beam} \cdot \sqrt{B_{tor}^2 + B_{pol}^2}$ where the Lorentz field leads to wavelength separation of the MSE pattern of:

$$\Delta\lambda_L = \frac{3}{2} e \cdot a_0 \cdot \frac{\lambda_0^2}{h \cdot c} \cdot E_{Lorentz}$$

For a toroidal field of 5.2 Tesla and a DNB energy of 100keV/amu the resulting separation of the Stark components is 6.6 Å (cf. Fig.10). The expected accuracy for the wavelength splitting is of the order 0.2 % at r/a=0.3. The high accuracy of the splitting is due to the fact that the MSE spectrum comprises 9 equidistant components and the statistical certainty is consequently improved.

In theory, if the toroidal field was known to an accuracy of better than, say 0.5 %, and diamagnetic effects could be excluded, it would be possible to deduce even the local pitch angles from the Stark splitting:

$$\Delta\lambda_L = \frac{3}{2} e \cdot a_0 \cdot \frac{\lambda_0^2}{h \cdot c} \cdot v_{beam} \cdot B_{tor} \sqrt{1 + \frac{B_{pol}^2}{B_{tor}^2}}$$

Close to the magnetic axis, where the poloidal field is approximately zero, the Stark splitting will provide a very accurate measurement of the toroidal field. In fact, changes of the total field and hence plasma pressure could be measured successfully at JET by this method during ICRH heating experiments (cf. reference 9).

MSE error analysis

The present study is based on simulated ITER DNB-MSE spectra, where the spectral noise level is determined by the fluctuations of the background signal representing the underlying continuum radiation level. This implies active modulation of the DNB and separation of active and passive components. Beam modulation schemes are been routinely used for example at the DIII-D CXRS system. There is, however a caveat with regard to stochastic occurrences of edge line emission, for example, during ELMy H-modes. Moreover, even a moderate DNB power level of about 2 MW, may, at least in principle, affect the overall ionisation balance, and therefore the neutral density background level and thus modify passive CX features.

The following figures show a blow-up of the MSE feature for the top-port periscope, and the derived parameters errors expressed by the 95% confidence intervals of the least-square minimisation routine.

An important feature of the parametrised MSE spectrum is a comprehensive atomic modelling, which reduces the number of free parameters to one common amplitude for the π-group, one for the σ-group, one common Stark splitting for all 9 components, and also one common width of all components. The finite beam divergence and ripple in the acceleration voltage lead to a broadening and slight asymmetry in the MSE pattern.

The spectral amplitude error at half-maximum is estimated to be about 2% at ρ=0.3. The amplitude error decreases towards the plasma boundary due to the exponentially increasing beam-strength.

The scheme of exploiting accurate line ratios from the MSE pattern relies crucially on the validity of the atomic modelling, and, moreover on the accurate experimental assessment of the optical transfer characteristics. In the case of the top-port periscope

changes of about 30% and for the lower equatorial port changes of about 12% are expected. The feasibility of the proposed ratiometry hinges therefore on the calibration of the periscope characteristics, which need to be better than 1%. For this reason, proof of principle experiments need to be carried out on current machines.

6. Calibration:

In view of expected immediate changes in transmission optics during extended ITER pulses the absolute calibration of spectroscopic instruments is a major concern. Based on similar experiences at JET and other fusion experiments, it is proposed to make use of the plasma itself as a calibrations source and exploit well advanced atomic modelling of line-emission in order to establish absolute calibrations. In the case of Active Beam Spectroscopy it has been successfully proven that the combination of CXRS and BES will provide access to absolute ion densities. This technique not only allows instantaneous on-line calibration regardless of the actual status of the 'first mirror' but, equally important, it avoids potential errors sources in beam attenuation calculations (c.f. Ref.8) and reduces absolute density measurements to a line ratio measurement.

A further aspect is the elimination of unknown geometry factors since one single viewing line, and hence one common active emission volume, can be shared by two dedicated instruments for CXRS and BES respectively.

In the case of a single energy species negative-ion-source-DNB the two processes are described by:

Beam emission: $D(E) + e \rightarrow D^{*}(E) + e$

And the associated emitted photon flux:

$$\mathrm{I_{bes}(E)} = \frac{1}{4\pi}\mathrm{n_e}\cdot\mathrm{Q_{BES}}\cdot\int \mathrm{n_b(E)ds}$$

Charge Exchange Recombination: $He^{+2}(T) + D^{0}(E) \rightarrow He^{+,*}(T) + D^{+}(E)$

and the associated emitted photon flux:

$$I_{CXRS}(T) = \frac{1}{4\pi} n_z \cdot Q_{CXRS} \cdot \int n_b(E) ds$$

The deduced local ion density is then reduced to a mere ratio of line intensities and atomic emission rates

$$\frac{\mathrm{n_z}}{\mathrm{n_e}} = \frac{\mathrm{I_{CX}}\cdot\mathrm{Q_{BES}}}{\mathrm{I_{BES}}\cdot\mathrm{Q_{CX}}}$$

Since the detector sensitivity is wavelength dependent corresponding changes of calibration factors need to be taken into account. This is achieved by using the underlying continuum as common cross-reference. The line-of-sight averaged Z_{eff}

$$\frac{\mathrm{n_z}}{\mathrm{n_e}} = \frac{\mathrm{I_{CX}}}{\mathrm{I_{BES}}}\cdot\frac{\mathrm{Q_{BES}}}{\mathrm{Q_{CX}}}\cdot\frac{\mathrm{I_{cont}}(\lambda_{\mathrm{BES}})}{\mathrm{I_{cont}}(\lambda_{\mathrm{CX}})}\cdot\frac{\lambda_{\mathrm{BES}}}{\lambda_{\mathrm{CX}}}\cdot\frac{\mathrm{g_{ff}}(\lambda_{\mathrm{CX}})}{\mathrm{g_{ff}}(\lambda_{\mathrm{BES}})}$$

value as deduced from the visible free-free-bremsstrahlung level, is the same for a CVI CX spectrum at 5290 Å or a D-alpha BES spectrum at 6561 Å. This method of combining BES and continuum radiation has been used successfully at TEXTOR for the deduction of absolute C^{6+} and Ne^{10}+ ion densities.

7. Arguments for the preference of either a negative ion source based DNB or a positive ion source based DNB

Historically, the specification of an optimum beam energy for an Active Beam based diagnostic for nuclear fusion plasmas has gradually decreased from the MeV range, which would give the optimum response for double-charge-exchange with slowing down alpha particles, towards the presently considered optimum neutral beam energy for a CXRS diagnostic which lies around 100 keV/amu (cf. Ref.8). Since positive ion sources systems rapidly loose their neutralisation efficiency beyond 100 keV/amu, considerable effort has been placed over the last decade in the development of high-power negative ion sources. These sources are potentially powerful candidates for plasma heating in an environment where high plasma densities requires high beam energies providing sufficient penetration for core heating. At the LHD experiment a negative ion source beam has been developed as a heating source. Recently achieved parameters are: 4.4 MW at 180 keV (H^0) focused on a spot size of 85 by 200 mm at a distance of 17 m. This corresponds to a neutral current density of 46 mA/cm^2.

The currently developed scheme for CXRS/BES is a 100 keV/amu negative ion based neutral beam with a current of about 22 A[16]. The envisaged operational scheme is having a sequence of several pulses during extended ITER pulses. Each pulse may be modulated for background suppression.

In view of new data[17] on improved focusing capabilities of positive ion sources compared to earlier data the discussion of whether a positive or a negative ion source would be a preferable solution for a ITER DNB has been restarted.

For a maximum spectral SNR and ITER densities of the order $10^{20}m^{-3}$ a probe beam energy in the range 80 to 120 keV/amu would be acceptable (cf. Fig.14 and Ref.8). Comparing the merits of either a negative or positive ion source DNB one has to consider several aspects.

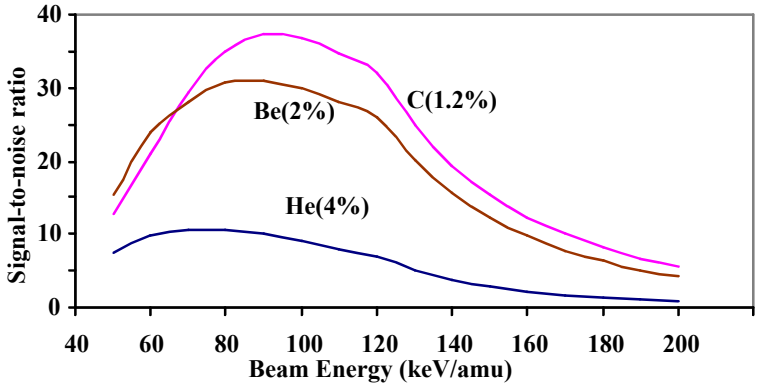

Fig.14 SNR for HeII, CVI and BeIV CX spectra at half-maximum for a 22A, neutral current negative ion diagnostic beam at an electron line density of $1.45 \cdot 10^{20} m^{-2}$ .The beam current is assumed to be a constant for the entire energy range. The shape reflects the trade-off between resonant charge capture and gain in beam penetration with beam energy (cf. Ref.8).

Starting with the physics aspects:

Clearly, a single energy species neutral beam, that is a negative ion source neutral beam, is simpler to evaluate in terms of ion density deduction from analysed CX intensities. The fact that only one component contributes actively to a measured CX spectrum makes any refined monitoring of species mix, energy dependent beam divergences etc. redundant.

However, since BES is considered to be an absolute must for calibration, the beam characteristics, such as species mix and local beam strength, will have to be monitored anyway. At TEXTOR, where a positive ion source neutral heating beam is

[16] E. Di Pietro et al. FUSION ENGINEERING AND DESIGN **56**-7: 929-934 OCT 2001
[17] H.Falter, EFDA Contract 00/559, December 2001

used as probe beam, this on-line self calibration technique has proven to work reliably (cf. Ref. 1).

There is another potential physics advantage linked to a positive ion source DNB which has to be included in the arguments:

At JET successful doping experiments were carried out, where a small amount of helium was added to the beam fuelling gas[18], acting as a tracer material. This allows the measurement of a number HeI lines distributed over the visible wavelength range along the beam path. By this method relative calibration factors between adjacent radial channels could be successfully established. The method is thus an alternative to the D-alpha-BES plus continuum cross-calibration technique as described in section 6. Realistic performance studies for ITER conditions are awaited in the near future.

Comparing the physics benefits of the two possible ion source DNB one has to consider achievable spectral measuring capabilities of the two competing alternatives: A 80 kev/amu positive ion source DNB compared to a 100keV/amu negative ion source DNB.

The spectral signal-to-noise ratio, or figure of merit (cf. Reference 8) reduces in a comparison of the two systems to:

$$\frac{S}{N}(\lambda_{1/2}) \propto \frac{I_n \sigma_{CX} \exp\{-\int dr n_e \sum_z c_z \sigma_{z,stop}\}}{w_\perp}$$

Here the exponential factor represents the energy dependent beam attenuation, I_n, the neutral current, σ_{cx}, the cx emission cross-section, σ_{stop} the beam stopping cross-section, c_z the impurity ion concentration, n_e the electron density and finally $w_\perp$ the 1/e radius of the neutral beam in the direction perpendicular to the line of sight. Note that only the full energy-component is shown for this ratio. Half and third energy components contribute about 10% to the CX signal due to the stronger attenuation.

The following two tables summarise beam characteristics and the main spectroscopic performance numbers for the reference radius r/a=0.3, reference electron line-density along the beam path of $1.45 \cdot 10^{20} m^{-2}$ and reference concentrations of He(4%), C(1.2%) and Be(2%) respectively.

	Positive Ion Beam (Ref.17)	Negative Ion Beam (Ref.16)
Beam divergence (mrad)	2.6, 3.5, 4.3	5
Achievable Current Density in focal position (mA/cm^2)	183, 23, 29	70
Beam 1/e-radius (m)	0.042, 0.056, 0.07	0.10
Species mix	0.85:0.075:0.075	1:0:0
Peak power (MW)	1.9	2.2
Voltage (kV)	160 D^0	100 H^0
Total neutral current (A)	12	22
Ion Dump Load (MW)	7.7	2.2
Power Input (MW)	9.6	4.4
Neutralisation efficiency	20 %	50 %

[18] K-D.Zastrow et al. 4th Meeting of ITPA Topical Group on Diagnostics, Padua, February 2003.

	Positive Ion Beam (80keV/amu)	Negative Ion Beam (100keV/amu)
Attenuation (r/a=0.3)	0.016, 0.0019,0.00039	0.026
σ_{cx} (HeII)($10^{-22}m^2$)	3.77, 16.1,15.9	1.89
σ_{cx} (CVI)($10^{-22}m^2$)	25.5, 35.6,17.9	16.02
σ_{cx} (BeIV)($10^{-22}m^2$)	14.4, 31.5,22.7	8.42
Spectral SNR (HeII @ρ=0.3)	18	12
Spectral SNR (CVI @ρ=0.3)	58	53
Spectral SNR (BeIV @ρ=0.3)	51	43

In terms of spectral signal-to-noise a boost of about 50 % for He^{+2} (20% for Be^{+4} and 10% for C^{+6}) is expected for a positive ion source DNB with its lower divergence. The biggest effect is seen for HeII where the cx emission rates increases rapidly towards lower beam energies. This implies that even in the very plasma centre (r/a=0.1) helium ash measurements would be a realistic prospect with a SNR>5.

Also in view of its doping capability, it must be concluded that a physics choice would rather favour a positive ion source. The main caveat is power-load handling and the verification of the focussing capability.

It remains to discuss briefly the **more technical aspects of the two alternative beam sources**. There are several issues to consider.

a) **Suitability for high duty cycle operation.** Ultimately, a maximum diagnostic coverage is required for the DNB operation providing a maximum of information on extended ITER pulses (>1000s). A duty cycle of about 50%, e.g., 10s on-time followed by 10s off-time appears presently to be a realistic number (this applies to a negative DNB with power loads <5MW)..
b) **Neutralisation efficiency and cooling requirements for ion dumps.** Neutralisation efficiency for positive ion sources are typically 20%, that is 80% of the electric power has to be absorbed by the ion dump structure. By contrast, negative ion sources can achieve neutralisation efficiencies up to 60%.
c) **Focussing capability.** Nominally positive ion sources could reach a factor of 2 lower beam divergences (2.5mrad compared to 5mrad). However, this number refers to individual beamlets. The entire assembly of several beamlets needs to be focussed into the plasma core. A pilot experiment is required to prove that an overall beam divergence of that order can be achieved.
d) **Space requirements and volume.** The DNB needs to be accommodated in its reserved envelope. A positive ion source may be smaller, and therefore less space required. The distance of a positive ion source beam to plasma centre can be reduced to 16m compared to 20m.
e) **Blanket aperture.** The latest discussions have emphasised the need for a DNB reaching the plasma centre. This implies sharing of a common port

plug of DNB and HNB in section 4 of ITER. See also report[19] and Fig.15. A low divergence will obviously be a preferred choice.

f) **Development needs.** Obviously any test-bed results with respect to achievable power levels, beam divergence and focussing capability will be helpful. A further aspect is the need of high-quality voltage stabilisation to ensure sensible MSE evaluation.

In summary: Lower divergence, higher neutral current density and therefore higher signal levels and also technically smaller blanket apertures support a positive ion source rather than a negative ion source DNB. This is achieved at the cost of substantially higher ion-dump-power levels and lower efficiency. Realistic operation lengths and duty cycles for long pulses for both systems need to be established.

8. Physics issues for a shifted DNB reaching the magnetic axis

The necessity of port sharing of the ITER Heating Neutral Beam and the DNB has led to an offset allocation of the DNB implying that the actual magnetic axis could not be reached. This solution appeared to be acceptable in view of the originally far more down-beat prospects of the performance of a DNB based CXRS diagnostic (see also Ref.8). In the course of the last years substantial steps for performance

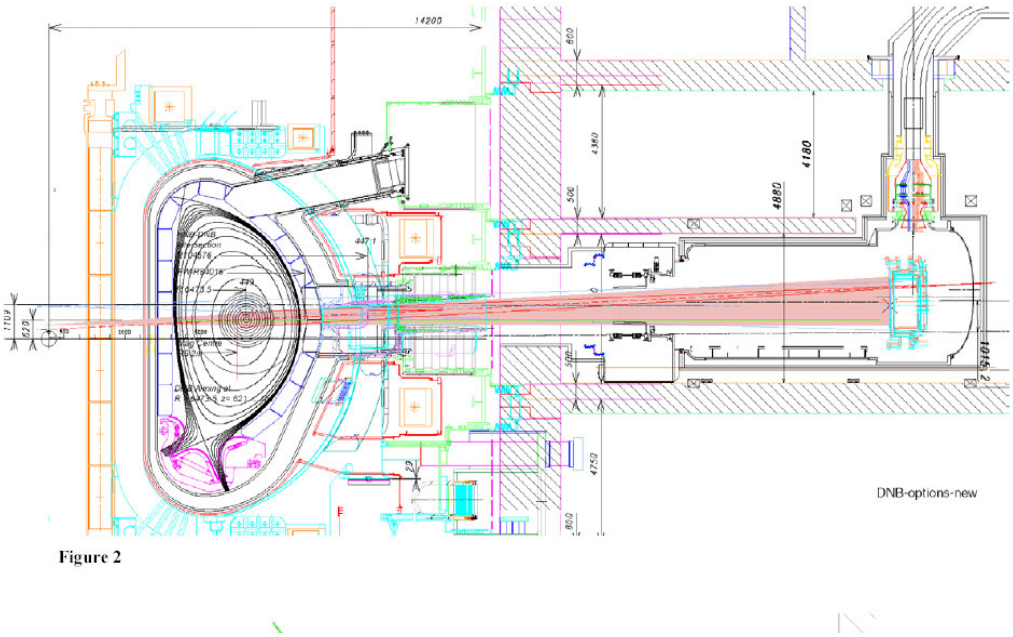

Fig.15. Tilted DNB reaching the ITER magnetic axis region (cf. Chris Walker)

improvements have been discussed and also accepted as a viable proposal, which have led, for instance, to an expected Signal-to-Noise ratio of about 10 for helium ash-measurement at a minor radius of r/a=0.3. This was primarily the result of optimising

[19] Chris Walker, ITER Memorandum 55 MD 158 03-09-09 W 0.1

the viewing geometry and, more importantly, considering single high-étendue spectral instruments and cameras for each individual radial channel. In view of this positive development, frequently commented on concerns by the physics community were taken on board and it was decided to reopen the discussion[20].

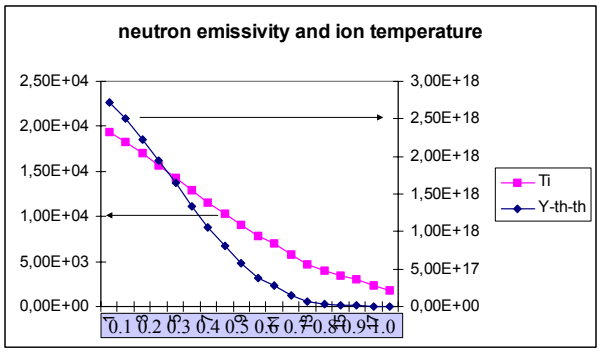

Fig.16 Simulated ITER thermal-thermal neutron profile and Ti profile

The crucial point is: Which physical process in the very core region, that is r/a<0.3, would make a central CXRS diagnostic indispensable, or highly recommendable? One obvious candidate is the fusion alpha production which has a characteristic half maximum at about r/a=0.3 (Fig.16). The need in this case is twofold. In the first instance, the non-linear temperature dependence of the thermal-thermal neutron rate make a highly resolved and accurate ion temperature profile very desirable. On the other hand, the recently proposed CXRS measurement of slowing-down fusion alphas, make it highly recommendable to study alpha populations in the very core. It must be admitted that the second argument is arguable since the proposal is still a development project. So, further theoretical studies as well as pilot experiments on present experiments are needed to backup this scheme.

A further issue is that in recent 'advanced scenario' tokamak operations with internal transport barriers steep ion temperature profiles are created and more attention is placed on the very core physics. In this context one has also to review critically the viability of complementary non-active, non-local diagnostic methods, which, in theory, may also provide central values from tomographic or other inversion procedures.

At the end of the day, the probability of ensuring global data consistency is much increased by a policy which favours a concerted approach to diagnostic coverage and any avoidable extrapolation into non-measured regions will be a draw-back.

9. Future Work

The main emphasis will be dedicated to a number of pilot experiments on present fusion devices addressing problems outlined above. In particular, the following subjects will have to be addressed:

a) First mirror-studies: Pilot experiments need to confirm predicted effects of coating of carbon or beryllium on metallic mirrors (e.g. molybdenium) and establish precise numbers on reflectivity and polarisation effects. More importantly, in situ assessment methods for the actual status need to be explored.

Active removal of coatings by high-power laser pulses techniques need to be explored. Possible schemes envisage also the combination of shutters in front of the first mirror and retro-reflectors mounted on its back, which

[20] M von Hellermann et al., 5th ITPA Meeting, St.Petersburg, 12 to 18 July 2003

could be used to measure polarisation characteristics for the entire periscope path and its components.

b) **Optimisation of instruments:** So far, the pre-dominant conceptual requirement was dedicated to an optimisation of helium-ash measurements by CXRS. The development of the diagnostic into a multi-tasking system with several instruments sharing common viewing lines and periscopes, needs further optimisation studies. For example, the development of multi-wavelength spectrometer assemblies cum camera, which allow the simultaneous recording of the three dominant CXRS wavelength regimes (cf. Fig.6) by one single spectrometer would reduce maintenance and simplify operation significantly.

c) **Detection limits on current machines:** The basis of our signal-to-noise studies are extrapolations from present CXRS systems on operating experiments to the ITER parameter range and recently developed high optical throughput instruments. A beam-modulation scheme is proposed for ITER to suppress a substantial background signal level introduced by plasma continuum radiation. Intensive background line-emissions, e.g. during ELM activities, require additional measures. This can be achieved by either optimised data-sampling schemes, which would allow exclusion of ELM time-windows, or alternatively, the inclusion of edge lines in a comprehensive spectral analysis procedure. The latter approach benefits greatly from advanced atomic modelling with precise wavelength and line-ratio predictions.

d) MSE ratiometry pilot experiments: The proposal for a combined evaluation of the MSE polarisation pattern by polarimetry and ratiometry, will have to be tested on present machines. At TEXTOR an ITER-geometry-like pilot experiment is prepared presently studying achievable accuracies. One essential part of this study will be the exploration of unpolarised continuum radiation for the assessment of polarisation dependent reflection properties.

e) **Development work on non-thermal distribution functions and spectral features:** This last subject encompasses both modelling of anisotropic slowing-down functions including fusion alphas and fast ion populations created by the ITER HNB system, and also verification of atomic modelling of CX capture in broad-band spectra. Experimentally, the accuracy of continuum background radiation measurements needs to be assessed, since the key issue of all non-thermal features is its discrimination from a broad-band background.